
[View Journal Online](#)
[View Article Online](#)

Synthesis, characterization, DFT, biological activities and molecular docking analysis of Schiff base ligand and its transition metal complexes

Minakshee Abhijit Todarwal ¹, Samina Karimkha Tadavi ², Rakesh Suresh Sancheti ¹ and Ratnamala Subhash Bendre ^{3,*}

¹ Department of Chemistry, Shri Neminath Jain Brahmacharyashram Karmvir Keshavlalji Harakchandji Abad Arts, Shriman Motilalji Girdharilalji Lodha Commerce and Shriman P. H. Jain Science College Chandwad, Maharashtra, 423101, India

² Department of Chemistry, Jashbhai Muljibhai Patel Arts, Commerce, and Science College, Bhandara, Maharashtra, 441904, India

³ School of Chemical Sciences, Kavayitri Bahinabai Chaudhari North Maharashtra University, Jalgaon, Maharashtra, 425002, India

* Corresponding author at: School of Chemical Sciences, Kavayitri Bahinabai Chaudhari North Maharashtra University, Jalgaon, Maharashtra, 425002, India. e-mail: bendrs@rediffmail.com (R.S. Bendre).

RESEARCH ARTICLE



doi 10.5155/eurjchem.15.2.128-142.2543

Received: 2 March 2024

Received in revised form: 27 March 2024

Accepted: 27 April 2024

Published online: 30 June 2024

Printed: 30 June 2024

KEYWORDS

DFT

Molecular docking

Biological activities

Plasmodium falciparum

Transition metal complexes

Salen type Schiff base ligand

ABSTRACT

In this study, we synthesized a tetradentate Salen type Schiff base ligand ($H_2L = 6,6'-((4\text{-chloro-1,2-phenylene})\text{bis}(\text{azanylylidene}))\text{bis}(\text{methanylylidene}))\text{bis}(2\text{-isopropyl-5-methyl-phenol})$) containing N_2O_2 donor atoms and its analogous transition metal complexes, namely CoL , NiL , CuL , and ZnL . The ligand was prepared through the condensation reaction of 3-isopropyl-6-methylsalicylaldehyde and 4-chloro-1,2-phenylene diamine. Various spectroscopic methods viz. FT-IR, UV-Vis, 1H - and ^{13}C -NMR, ESI-MS, and elemental analysis were utilized to elucidate the synthesized compounds. The free ligand coordinates with the metal ions in 1:1 molar ratio. The bactericidal investigations of the compounds were performed against *S. aureus*, *S. pyogenes*, *E. coli*, and *P. aeruginosa*. Antimalarial, anti-inflammatory and antioxidant activities were also studied. The DFT study was performed to optimize the geometry and evaluate the chemical reactivity parameters. The molecular docking investigation was performed to evaluate the binding interactions and binding energy of the synthesized compounds against cysteine protease SpeB and lactate dehydrogenase receptor proteins. This investigation established a good correlation between theoretical and practical outcomes.

Cite this: *Eur. J. Chem.* 2024, 15(2), 128-142

Journal website: www.eurjchem.com

1. Introduction

Pharmaceutical design approaches often employ a chemical method that assembles two or more molecules to form novel molecules with unique biological attributes. Biochemical synthesis, anticancer, antibacterial and anti-inflammatory properties, along with the various catalytic attributes of Schiff bases, allows them to be distinctive among the compounds [1]. Over the past two decades, a great deal of research has been reported on N_2O_2 donor ligands and their metal complexes, highlighting their enormous range of applications [2-12]. These compounds have attracted the attention of many researchers due to their peculiar structures, composed of two nitrogen and two oxygen atoms, together with their affluent coordination chemistry [13]. This arrangement offers an appealing geometry to ligands for interacting with metal ions through four active sites. These Salen-type Schiff base ligand compounds are generally applicable for biological and industrial purposes, due to their attractive physical and chemical attributes [14]. These compounds readily react with almost all metal ions present in the periodic table owing to this quality; they act as crucial

building blocks of coordination chemistry. Furthermore, these Salen-type Schiff base ligands form more stable metal complexes with various oxidation states [15]. The great applicability of Salen-based complexes in various realms is due to their elevated binding constant, $\log K > 20$ [16]. Metal complexes are believed to affect biological systems through inhibition of enzymes, elevated lipophilicity, interaction with endocellular biomolecules, altered cell membrane characteristics, stoppage of cell processes, and many other mechanisms. The goal of metal complexes is to modify the physiochemical attributes due to a comprehensive assortment of coordination spheres, oxidation states, redox potentials, and ligand configurations. Thus, the biological features of ligands and their metal complexes are extensively influenced by complexation [17]. The most important cause that leads to an improvement in the chemical stability and basicity of metal complexes is the existence of imine bonds [18]. Halo atoms containing ligands have been widely investigated by many researchers due to their wide range of applications in pharmacology, biological chemistry, and physiology [19]. Furthermore, these halogenated Schiff base ligands demonstrate elevated

binding affinity, oral absorbability, and membrane permeability [19,20]. Despite significant advances in the field of biomedical research, malaria, a parasitic ailment, still persists as an unresolved challenge for humans. The World Health Organization (WHO) reported an estimated 619,000 malaria-related deaths worldwide in 2021 [21]. Among the malaria parasites, *Plasmodium falciparum* is responsible primarily for the stern form of malaria. Due to the emergence of drug-resistant parasites, several antimalarial drugs have become ineffective. This condition highlights the need to discover new therapeutic drugs to combat malarial parasites [22]. Similarly, as a consequence of the overuse and misuse of antibiotics, resistant bacterial strains have emerged. As a consequence of antimicrobial resistance (AMR), 4.95 million deaths occurred in 2019. Due to the rise of antibiotic resistant infections, there is an imperative need to develop new antibiotics. Since the last decades, researchers have applied various approaches to improve the efficacy of antibiotics; among them, drugs containing metal ions are a probable way, which has demonstrated high efficacy against a variety of bacterial strains [23]. The production of reactive oxygen species (ROS) causes a variety of abnormalities in the physiological function of the human body, resulting in a number of cancers by bursting the number of proteins and lipids in cells [24,25]. For the treatment of such abnormalities in the human body, antioxidants were employed. Consequently, there is an essential requirement to develop promising drugs with high antioxidant and anticancer efficacy [24]. After an extensive literature survey focused on the antimalarial efficacy of N_2O_2 donor Salen-type Schiff base ligands and their transition metal complexes, a small number of relevant reports were documented. Recently, Dalal *et al.* explored the antimalarial efficacy of the N_2O_2 donor Schiff base ligand and its aryl tellurium complexes [22]. This approach distinguishes our research by presenting an antimalarial aspect with a new Salen-type Schiff base ligand moiety. However, several studies have demonstrated the antimicrobial, anti-inflammatory, and antioxidant effectiveness of Salen-type Schiff base ligands and their transition metal complexes [24,26-28]. On the basis of the analysis of the aforementioned literature, the wide range of applications exhibited by Salen-type Schiff base ligands and their metal complexes in drug development and biological activities led us to synthesize a novel Salen-type Schiff base ligand and its metal complexes.

The purpose of our research is to explore the bioefficacy of the synthesized compounds, especially their antimalarial efficacy along with their antibacterial, antioxidant, and anti-inflammatory potential, by synthesizing N_2O_2 donor quadridentate salen Schiff base ligand, 6,6'-(((4-chloro-1,2-phenylene)bis(azanylylidene))bis(methanylylidene))bis(2-isopropyl-5-methylphenol), (H_2L), and its corresponding transition metal complexes such as CoL, NiL, CuL, and ZnL. DFT investigations were performed to predict the geometry, HOMO-LUMO energy gap, dipole moment, and chemical reactivity parameters. Additionally, molecular docking investigations were performed on the cysteine protease SpeB and the lactate dehydrogenase receptor protein to determine the binding score and binding interactions of compounds.

2. Experimental

2.1. Materials and instrumentation

High purity chemicals such as 3-isopropyl-6-methyl salicylaldehyde, 4-chloro-1,2-diaminobenzene, chloroform, ethanol, methanol, triethylamine, and metal salts such as cobalt acetate tetrahydrate, nickel acetate tetrahydrate, copper acetate, and zinc acetate dihydrate were obtained from Sigma Aldrich. All reagents and chemicals were of research grade and were utilized without further purification. Elemental analysis (CHN) of the synthesized compounds was conducted using the

Thermo Finnigan elemental analyzer. Fourier transform infrared (FT-IR) spectra of the compounds were recorded using a Shimadzu FT-IR-8400 spectrometer. Electrospray ionization mass spectrometry (ESI/MS) spectra of the synthesized compounds were acquired on a Waters Micromass Q-ToF micro instrument employing chloroform as the solvent. Proton nuclear magnetic resonance (1H NMR) and carbon-13 nuclear magnetic resonance (^{13}C NMR) spectra of the ligand were obtained using a Bruker Advance III spectrometer operating at 500 MHz.

2.2. Synthesis of Salen type Schiff base ligand (H_2L)

For the synthesis of the Schiff base ligand (H_2L), 3-isopropyl-6-methylsalicylaldehyde (2 mmol) dissolved in methanol was slowly added dropwise to a methanolic solution containing 4-chloro-1,2-phenylenediamine (1 mmol) with continuous stirring. The resulting yellow reaction mixture was refluxed at 60 °C for 3 hours. The progress of the reaction was monitored using thin layer chromatography (TLC) with *n*-hexane:ethyl acetate (10%) solvent system. The resulting yellow solid was then collected, washed with cold methanol, and subjected to recrystallization in ethanol, followed by vacuum drying [1,2].

6, 6'-(((4-Chloro-1, 2-phenylene)bis(azanylylidene))bis(methanylylidene))bis(2-isopropyl-5-methylphenol) [H_2L]: Color: Yellowish orange. Yield: 85%. 1H NMR (500 MHz, $CHCl_3$, δ , ppm): 13.68 (s, OH, 2H), 8.95 (s, CH=N, 2H), 7.29-6.63 (m, Ar, 7H), 2.48-2.45 (s, CH₃, 6H), 1.35-1.32 (m, CH, 2H), 1.22-1.21 (d, 4CH₃, 12H). ^{13}C NMR (125 MHz, $CHCl_3$, δ , ppm): 161.2, 160.87, 160.63, 159.26, 141.79, 139.43, 139.22, 134.8, 133.9, 133.26, 133.17, 130.5, 130.29, 127.49, 121.39, 120.96, 120.91, 118.03, 116.76, 116.51, 26.44, 26.31, 26.01, 22.45, 22.26, 19.02, 18.97, 17.92. FTIR (KBr, ν , cm^{-1}): 3446 (O-H), 1548 (C=N), 1423 (C=C), 1288 (C-O). UV-Vis ($CHCl_3$, λ_{max} , nm): 290, 340. MS (EI, m/z (%)): 465.03 (M^+ , 100). Anal. calcd. for $C_{28}H_{31}ClN_2O_2$: C, 72.63; H, 6.75; N, 6.05. Found: C, 72.20; H, 6.68; N, 5.33%.

2.3. Synthesis of metal complexes

The CoL, NiL, CuL, and ZnL complexes of the ligand (H_2L) were synthesized by combining a boiling methanolic solution of the ligand (1 mmol) with a hot methanolic solution of the corresponding metal salts (1 mmol). The resulting reaction mixture was stirred and refluxed for duration of 3 hours. Subsequently, the colored precipitates of the complexes were filtered, washed with various nonpolar solvents, and dried under vacuum conditions [1].

[CoL] complex: Yield: 72 %. Colour: Dark brown. M.p.: > 300 °C. FT-IR (KBr, ν , cm^{-1}): 1529 (C=N), 1354 (C=C), 1199 (C-O), 574 (M-O), 418 (M-N). UV-Vis ($CHCl_3$, λ_{max} , nm): 275, 352, 410. MS (EI, m/z (%)): 519.12 (M^+ , 100). Anal. calcd. for $C_{28}H_{29}ClCoN_2O_2$: C, 64.68; H, 5.62; N, 5.39. Found: C, 64.52; H, 5.71; N, 5.22%.

[NiL] complex: Yield: 71 %. Colour: Reddish brown. M.p.: > 300 °C. FT-IR (KBr, ν , cm^{-1}): 1533 (C=N), 1355 (C=C), 1193 (C-O), 549 (M-O). UV-Vis ($CHCl_3$, λ_{max} , nm): 265, 360, 470. 510. MS (EI, m/z (%)): 518.43 (M^+ , 100). Anal. calcd. for $C_{28}H_{29}ClNiN_2O_2$: C, 64.71; H, 5.62; N, 5.39. Found: C, 64.72; H, 5.60; N, 5.15%.

[CuL] complex: Yield: 74 %. Colour: Light brown. M.p.: > 300 °C. FTIR (KBr, ν , cm^{-1}): 1533 (C=N), 1354 (C=C), 1192 (C-O), 591 (M-O), 418 (M-N). UV-Vis ($CHCl_3$, λ_{max} , nm): 283, 359, 550. MS (EI, m/z (%)): 523.22 (M^+ , 100). Anal. calcd. for $C_{28}H_{29}ClCuN_2O_2$: C, 64.11; H, 5.57; N, 5.34. Found: C, 63.92; H, 5.72; N, 5.08%.

[ZnL] complex: Yield: 74 %. Colour: Yellow. M.p.: > 300 °C. FTIR (KBr, ν , cm^{-1}): 1541 (C=N), 1357 (C=C), 1192 (C-O), 545 (M-O), 418 (M-N). UV-Vis ($CHCl_3$, λ_{max} , nm): 263, 310, 415. MS (EI, m/z (%)): 526.38 (M^+ , 100). Anal. calcd. for $C_{28}H_{29}ClZnN_2O_2$: C, 63.89; H, 5.55; N, 5.32. Found: C, 63.04; H, 5.66; N, 4.96%.

2.4. Antibacterial activity assay

In vitro antibacterial activity assays were conducted on synthesized compounds employing the broth dilution technique, following the protocols outlined by the National Committee for Clinical Laboratory Standards (NCCLS), against Gram-negative strains *E. coli* (MTCC 443) and *P. aeruginosa* (MTCC 1688), as well as Gram-positive strains *S. aureus* (MTCC 96) and *S. pyogenes* (MTCC 442). The compounds were initially prepared at a stock solution concentration of 2000 μM , which was then further diluted at concentrations of 500, 250, and 125 μM for the preliminary bactericidal assessment. Active compounds identified in the initial screening were subjected to additional dilution steps to achieve concentrations of 100, 50, 25, 12.5, 6.25, 3.125, and 1.5625 μM . The minimum inhibitory concentration (MIC), defined as the highest dilution showing 99% inhibition, was determined. The concentration of bacterial inoculums was maintained at 1×10^8 organisms/mL. Tubes devoid of antibiotics were promptly subcultured onto appropriate growth medium plates to confirm microbial viability. The incubation of the microbial samples was carried out overnight at 37°C, with subsequent observation of growth. The MIC was recorded, indicating the minimum concentration at which the organism's growth is inhibited. The effects of solvents on strain growth were negligible, whereas the size of the inoculum exerted a significant influence. Ampicillin served as the standard drug, while both DMSO and distilled water were used as negative controls, and antibiotics were used as positive controls [29,30].

2.5. Antimalarial activity assay

In vitro antimalarial evaluations of the synthesized compounds were performed using 96-well microtiter plates, with slight modifications to the Rieckmann *et al.* microassay protocol [31]. The malarial strain *Plasmodium falciparum* (3D7) was maintained in RPMI 1640 medium supplemented with 25 mM HEPES, 1% D-glucose, 0.23% sodium bicarbonate, and 10% heat-inactivated human serum. After being treated with 5% D-sorbitol, the asynchronous malaria parasite *Plasmodium falciparum* was synchronized to produce cells that were infested during the ring stage. Jaswant Singh Bhattacharya (JSB) stain was used to determine initial ring stage parasitemia of 0.8 to 1.5% at 3% hematocrit in a whole quantity of 200 μL of medium RPMI-1640 for the investigation and was persistently sustained with 50% RBC (O⁺ve). In DMSO solvent, stock solutions of 5 mg/mL of the synthesized compounds were prepared with culture medium. To produce a final concentration (at five-fold dilutions) ranging from 0.4 to 100 g/mL in a duplicate well with parasitized cell preparation, the samples were diluted in a 20-L volume and applied to the test wells. In a candle jar, the culture plates were kept at 37 °C for incubation. Thin blood smears from each well were produced and then stained with JSB stain immediately after 36 to 40 hours of incubation. To observe the maturation of ring-stage parasites into trophozoites and schizonts, we observed the slides microscopically in the presence of different concentrations of the test samples. The amount of concentration that inhibits schizont formation was taken as the minimum inhibitory concentration. Here, quinine was used as a standard drug [30].

2.6. Anti-inflammatory activity assay

The *in vitro* anti-inflammatory activity of the synthesized compounds was investigated using the human red blood cell (HRBC) stabilization method [32]. Fresh blood was collected in a heparinized tube to prevent coagulation from a healthy human being. An identical volume of collected blood was combined with a sterilized Alsever's solution. Thereafter,

centrifugation of blood for 20 minutes at 3000 rpm was carried out to separate out the packed cells. These packed cells were thoroughly washed with isosaline (0.85% solution, pH = 7.2), and a 10% v/v suspension of isosaline was made. Then, this HRBC suspension was used to investigate the anti-inflammatory capabilities of the compounds. To perform the assay, 1 mL of sample with a concentration of 400 $\mu\text{g}/\text{mL}$ and 1 mL of diclofenac sodium in a hypo saline solution (0.25% NaCl) solution were combined separately with 1 mL of phosphate buffer (0.15 M, pH = 7.4), 2 mL of hyposaline (0.36%), and 0.5 mL of HRBC suspension. The entire analysis mixture was incubated at 37 °C for 30 minutes and then centrifuged at 3000 rpm for 20 minutes. The supernatant liquid obtained was decanted after the centrifugation process and the hemoglobin concentration in the supernatant solution was measured with a spectrophotometer set to 560 nm [33]. When the hemolysis produced in the control was assumed to be 100%, the percentage of hemolysis was estimated. This entire testing process was performed in triplicate to ensure the accuracy of the results. The % of HRBC membrane protection was measured using Equation 1 [34].

$$\% \text{ Protection} = 1 - \frac{\text{Absorbance of sample}}{\text{Absorbance of control}} \times 100 \quad (1)$$

2.7. Antioxidant activity assay

A microplate reader (BioTek Synergy HTX) was used to assess the antioxidant potential of the synthesized compounds in 96-well plates. The probe mixture in each well consists of 100 μL of 0.5 mg/mL concentration of the tester, to which 100 μL of 2,2-diphenyl-1-picrylhydrazyl (DPPH) solution in ethanol was mixed. The plate was agitated for 2 minutes, then enclosed and incubated at 37°C for 30 min. The absorbance of a mixture of synthesized compounds was determined using a microplate reader at 517 nm [35]. Each test solution was set in triplicate and the mean absorbance was calculated. L-ascorbic acid was used as a positive control. The inhibition of DPPH was calculated using Equation 2 [36].

$$\% \text{ Inhibition of DPPH} = \frac{C-S}{C} \times 100 \quad (2)$$

C = Absorption of the control and S = Absorption of the sample.

2.8. Molecular docking

The docking investigation was performed using the Schrodinger Glide (SP-docking) module [37]. *Plasmodium falciparum* lactate dehydrogenase inhibitors and cysteine protease SpeB structures were obtained from the Protein Data Bank (PDB) with accession codes 1CET [38] and 4RKX [39] (<https://www.rcsb.org/>). The restored protein structures were prepared by the "protein preparation wizard" panel [40]. In the primary stage of processing, the bond sequence was assigned, missing hydrogen was added, and the missing side chains and loops were modified. In the final refinement phase, to obtain an absolute energetic optimization, with the RMSD (root mean square deviation) of the heavy atoms set to 0.3 Å, the OPLS3 force field [41] was used. The 3D geometry of the synthesized compounds was prepared with the LigPrep panel [42]. The ionization state of each ligand structure was established at a physiological pH of 7.2±0.2. The active site grid was assigned by incorporating the related ligand into the crystal structure and employing the default dimension box. Lastly, the molecular docking investigation was carried out using Schrodinger's glide, in which the ready minimum energy 3D structure of the ligands and the receptor grid file were loaded into Maestro's work area and the ligands were docked using the extra precision (SP) docking methodology [43-46].

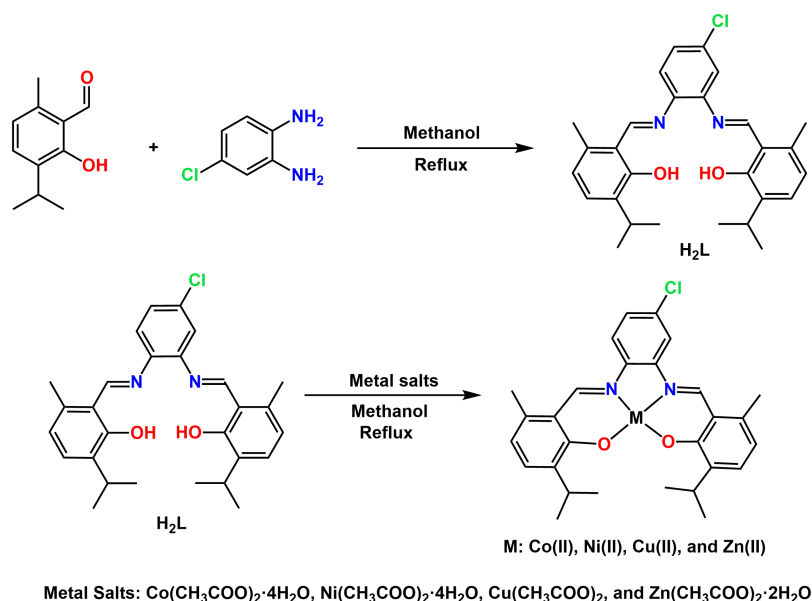


Figure 1. Synthesis of ligand and metal complexes.

2.9. Computational methods

To explore the molecular attributes of the synthesized compounds, full geometry optimization calculations were performed. Using the Avogadro software [47], the atomic coordinates of the synthesized compounds were built [48], and then further processed to produce an ORCA input file for comprehensive optimization of molecular geometry. Time-dependent density functional theory (TD-DFT) geometry optimizations were executed by B3LYP as a functional with 6-311G(d,p) and 6-311+G(d,p) basis set in the gas phase [49-52] using the ORCA program package (version 4.0.1) [53]. The geometry of the complexes was optimized with the B3LYP functional, which is used to predict the geometric attributes of transition metals due to its elevated accuracy [54,55]. Natural bond orbital (NBO) calculations were carried out on gas phase optimized compounds [56].

3. Results and discussion

The condensation reaction of 4-chloro-1,2-phenylene diamine (1 mmol) with 3-isopropyl-6-methyl salicylaldehyde (2 mmol) in methanol formed a yellow Salen-type Schiff base ligand (H_2L) (Figure 1). Furthermore, the CoL , NiL , CuL , and ZnL complexes of ligand were prepared by refluxing the equimolar (1:1) amount of ligand with analogous metal salts in methanol with constant magnetic stirring. The precipitates obtained were collected and filtered. The Schiff base ligand exhibited solubility in chloroform, dichloromethane, and acetone, whereas the metal complexes exhibited solubility in polar solvents such as DMF, DMSO, methanol, and ethyl acetate, etc.

3.1. Characterization of compounds

The ^1H and ^{13}C -NMR spectra of the H_2L compound were carried out using a chloroform solvent. In the ^1H -NMR spectrum, a singlet peak corresponding to the hydroxyl group (OH) is observed at δ 13.68 ppm. Additionally, the characteristic peak of the azomethine ($\text{HC}=\text{N}$) proton is detected at δ 8.95 ppm, while merged peaks attributed to aromatic protons are observed in the range of δ 7.29-6.63 ppm. The peak observed at δ 1.22-1.21 ppm corresponds to the aliphatic methyl protons of the ligand. In contrast, the peak attributed to aromatic methyl

protons is detected at δ 2.48-2.45 ppm. Aliphatic CH protons exhibit a multiplet pattern, appearing in the range of δ 1.35-1.32 ppm. The ^{13}C -NMR spectra of the ligand also give confirmation by demonstrating distinctive peaks of azomethine carbon 2 ($\text{C}=\text{N}$), 2 ($\text{C}-\text{OH}$) and 1 ($\text{C}-\text{Cl}$) at δ 161.2, 160.8, 160.63, 159.5, and 141.79 ppm, respectively. The aliphatic carbon peaks were visualized at δ 26.44-19.72 ppm [28].

The ESI-MS spectra of both the ligand and its metal complexes (CoL , NiL , CuL , and ZnL) were obtained using chloroform as the solvent. The mass spectra of compound H_2L revealed a molecular ion peak at m/z 463.95 (calculated as 463.02). Additionally, a fragment peak at m/z 338 [$\text{C}_{24}\text{H}_{22}\text{N}_2$] $^+$ emerged as a result of the loss of OH, Cl, CH_3 and $\text{CH}-(\text{CH}_3)_2$ ions. The CoL mass spectrum showed a peak at m/z 519.12, which matches the calculated value of 519.12. Furthermore, fragment peaks were observed at m/z 360, 301, and 285 due to the formation of [$\text{C}_{22}\text{H}_{17}\text{ClN}_2\text{O}$] $^+$, [$\text{C}_{20}\text{H}_{16}\text{N}_2\text{O}$] $^+$, and [$\text{C}_{20}\text{H}_{16}\text{N}_2$] $^+$ ions, respectively. The mass spectra of the NiL complex showed a peak at m/z 518.43 (calculated as 518.13). Furthermore, fragment peaks were seen at 462, 337, 301, and 283, which correspond to the formation of [$\text{C}_{28}\text{H}_{31}\text{ClN}_2\text{O}_2$] $^+$, [$\text{C}_{24}\text{H}_{22}\text{N}_2$] $^+$, [$\text{C}_{20}\text{H}_{16}\text{N}_2\text{O}$] $^+$, and [$\text{C}_{20}\text{H}_{16}\text{N}_2$] $^+$ ions, respectively. While the CuL complex ([$\text{C}_{28}\text{H}_{29}\text{ClCuN}_2\text{O}_2$]) had a mass peak at m/z 524.99 (estimated at 524.55), fragment peaks were found at m/z 338 and 301 for [$\text{C}_{24}\text{H}_{22}\text{N}_2$] $^+$ and [$\text{C}_{20}\text{H}_{16}\text{N}_2\text{O}$] $^+$, respectively. Similarly, the ESI-MS spectra of the ZnL molecule revealed a peak at m/z 526.38 (calculated as 526.98), with a fragment signal at m/z 462 resulting from zinc elimination. The mass spectra of all complexes clearly showed the coordination of the metal ions and ligands. Every compound's CHN investigation revealed a metal-ligand stoichiometry of 1:1, which is in line with the structural formula of the ML type.

The FT-IR spectrum of the ligand reveals a prominent ν_{OH} band at 3446 cm^{-1} . However, comparable metal complexes lack the ν_{OH} band in their IR spectra. The absence of a prominent ν_{OH} band in the spectra of metal complexes indicates complex formation. The characteristic imine band ($\nu_{\text{C}=\text{N}}$) was identified at 1548 cm^{-1} . However, in the complexes, the imine band was observed at lower wavenumbers ($1529\text{-}1541\text{ cm}^{-1}$) compared to the value of the ligand.

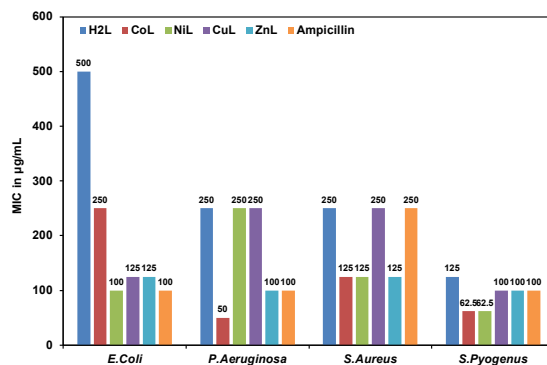


Figure 2. Graphical representation of antibacterial activity.

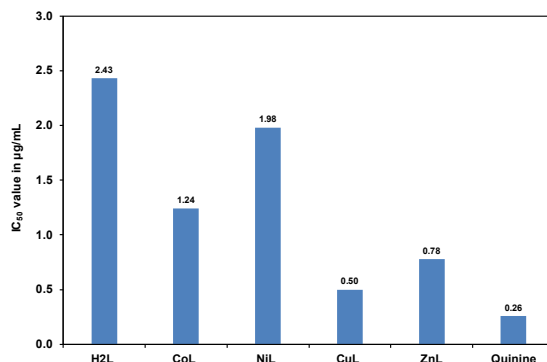


Figure 3. Graphical representation of the antimalarial activity of the synthesized compounds.

A new band at $591\text{-}418\text{ cm}^{-1}$ indicates the formation of M-N and M-O bonds, which confirms the formation of the complex. For every compound, the elemental analysis findings show a very good agreement with the theoretical values.

3.2. Antibacterial studies

Using the disc diffusion technique, the bacteriostatic efficiency of the obtained compounds was examined against Gram-negative strains *P. aeruginosa* and *E. coli*, as well as Gram-positive strains *S. aureus* and *S. pyogenes*. The findings show that as compared to the free ligand H₂L, all synthesized metal complexes (CoL, NiL, CuL, and ZnL) display improved bioefficacy. Figure 2 illustrates the graphical representation of antibacterial efficacy. The enhanced bactericidal activity of the complexes can be explained by using Overtone's concept of cellular permeability and Tweedy's chelation theory [57,58]. The overtone concept of cell permeability implies that liposolubility is an essential factor that influences the bactericidal activity of compounds. Thus, the lipid membrane of a cell promotes the passage of mainly lipid-soluble substances. Chelation reduces the polarity of metal ions by overlapping Schiff base orbitals and distributing the positive charge partially on metal ions. However, delocalizing π -electrons throughout the chelate ring enhances the lipophilicity of the complexes. Such a higher lipophilicity inhibits the continued development of bacteria and enhances the absorption of complexes into the lipid membrane. The diversity in the bioactivity of derived complexes with respect to various bacterial species depends on the variation in the cell permeability of bacteria or ribosomes of microorganism cells [58], diversity in the structure of the cell wall might lead to disparities in bactericidal vulnerability. Gram(+) bacterial species have thick cell walls consisting of multilayers of peptidoglycans and teichoic acid, while Gram(-) bacterial species have comparatively thin cell membranes containing a

few peptidoglycans enclosed through a secondary lipid membrane containing lipopolysaccharides and lipoproteins [59]. Antibacterial screening revealed that metal complexes are more harmful to Gram (+) species, particularly *S. pyogenes* (62.5-100 $\mu\text{g/mL}$), compared to Gram (-) species [1]. On the other hand, the Schiff base ligand complexes CoL and ZnL showed notable effectiveness against *P. aeruginosa* (50-100 $\mu\text{g/mL}$), while the NiL complex showed remarkable effectiveness against *E. coli* (100 $\mu\text{g/mL}$). The complexes derived exhibited varying degrees of antibacterial effectiveness, with the order ZnL > CoL > NiL > CuL > H₂L. The increased bactericidal efficiency of the ZnL complex may be related to its electron-rich character, which allows simple interaction with the DNA of bacterial strains using non-covalent interactions [58]. ZnL and CoL have better bactericidal properties as a result of their lower dipole moments. The decrease in polarity increases lipophilicity and hydrophobicity, resulting in a significant increase in antibacterial activity [60-64]. Table 1 compares the minimum inhibitory concentration (MIC) values of the complexes with analogous moieties, indicating the moderate to remarkable antibacterial activity of our compounds. It should be noted that the effectiveness varies depending on the type of bacteria.

3.3. Antimalarial activity studies

We used Rieckmann's microassay [70] to determine the *in vitro* antimalarial efficacy of the ligand and its metal chelates against the strain of *P. falciparum* (3D7), and then the findings were compared to quinine drugs. Figure 3 illustrates the antimalarial evaluation findings, expressed as half-maximum inhibitory concentration (IC₅₀) values.

Table 1. Many investigations are available in the literature for N₂O₂ donor Salen-Schiff bases and their antibacterial, antioxidant and anti-inflammatory activities.

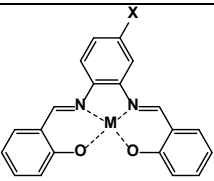
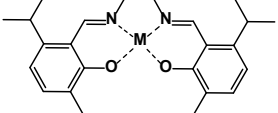
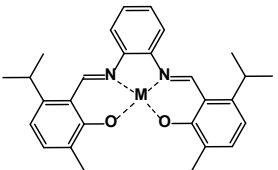
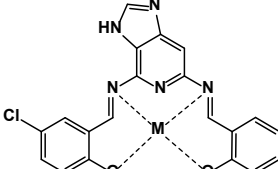
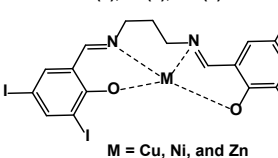
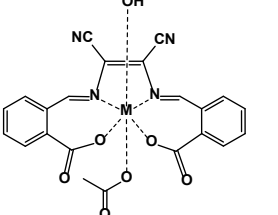
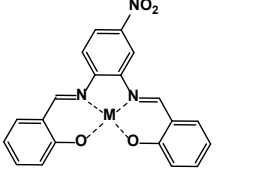
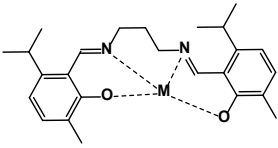
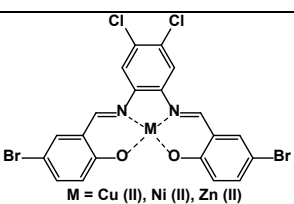
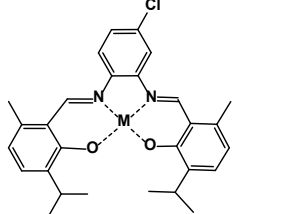
Structure of compounds	Antibacterial activity	Antioxidant activity	Anti-inflammatory activity	Reference
 <p>X = Cl, M = Cu (II) (3), Co (II) (4), Zn (II) (5)</p>	Co(II) complexes 4 and 7 are more active against <i>S. aureus</i> (27 and 22 mm, respectively), <i>K. pneumoniae</i> (23 and 17 mm, respectively).	-	-	[65]
 <p>X = Br, M = Cu (II) (6), Co (II) (7), Zn (II) (8)</p>	The Mn(III) complex is most active against <i>B. subtilis</i> , <i>S. aureus</i> , and <i>P. aeruginosa</i> , with MIC of 85, 87, and 70 µg/mL, respectively.	Ni(II) (14.21 µg/mL) and Cu(II) (15.29 µg/mL) complexes showed remarkable activity compared to BHT (16.50 µg/mL), and analogous to ascorbic acid (12.80 µg/mL) and α-tocopherol (12.80 µg/mL).	-	[28]
 <p>M = Mn (III), Co (II), Cu (II), Zn (II)</p>	Ni(II) and Cu(II) complexes demonstrated greater activity against all bacterial strains (63-102 µg/mL).	The Mn(II) (0.1124 µg/mL) and Cu(II) (0.1135 µg/mL) complex showed significantly higher antioxidant activity.	-	[66]
 <p>M = Mn (II), Co (II), Ni (II) and Cu (II)</p>	ZnL demonstrated a higher antibacterial potential towards <i>S. aureus</i> , <i>E. coli</i> , <i>K. pneumoniae</i> , and <i>P. aeruginosa</i> strains with an inhibition zone of 9 to 11 mm.	CuL (16.81±0.21 µM) exhibits the highest antioxidant activity, followed by the NiL (24.16±0.14 µM) complex.	ZnL (15.11±0.28µM) exhibits higher anti-inflammatory activity followed by CuL (24.16±0.25 µM)	[17]
 <p>M = Co (II), Ni (II), Cu (II) and Zn (II)</p> <p>M = Cu, Ni, and Zn</p>	CuL showed maximum activity against <i>E. coli</i> (15 mm) followed by ZnL (14 mm). The NiL and ZnL complexes showed maximum activity against <i>P. aeruginosa</i> (15 mm). For <i>S. aureus</i> (28 mm) and <i>B. cereus</i> (24 mm), ZnL showed maximum inhibition.	-	-	[26]
 <p>M = Co, Ni, Cu and Zn</p>	CoL, NiL, and CuL have comparable bactericidal activity against <i>S. aureus</i> and <i>K. pneumoniae</i> , however, ZnL has moderate antibacterial impact against all bacterial strains except <i>A. baumannii</i> .	-	CuL (289.68 µg/mL) and ZnL (209.24 µg/mL) demonstrated higher anti-inflammatory activity.	[67]
 <p>M = Co (II), Ni (II), and Cu (II)</p>	-	Nickel and copper complexes have higher antioxidant levels than the cobalt complex but lower than that of ascorbic acid.	The cobalt, nickel, and copper complexes showed effective anti-inflammatory activity compared to the sodium diclofenac drug.	[68]
 <p>M = Mn (II), Co (II), Ni (II) and Cu (II)</p>	The Mn(II) and Co(II) complexes possess better activity against <i>B. subtilis</i> and <i>S. aureus</i> . The Ni(II) complex shows superior antibacterial activity against all bacterial strains of <i>B. subtilis</i> , <i>P. aeruginosa</i> , and <i>S. aureus</i> .	Co(II) complex shows good antioxidant activity compared to the standard drug of butylated hydroxyl toluene (BHT).	-	[69]

Table 1. (Continued).

Structure of compounds	Antibacterial activity	Antioxidant activity	Anti-inflammatory activity	Reference
 <p>M = Cu (II), Ni (II), Zn (II)</p>	<p>NiL showed better activity against <i>S. aureus</i>, whereas ZnL was more active against <i>P. aeruginosa</i> and <i>S. pneumoniae</i>.</p>	<p>Cu complex (3), 0.498±0.20 mg/mL showed prominent antioxidant properties, followed by Ni complex (2) 0.517±0.20 mg/mL.</p>	<p>ZnL (4) has superior activity among all synthesized compounds 448.02±0.17 µg/mL.</p>	[1]
 <p>M = Co(II), Ni (II), Cu (II), and Zn (II)</p>	<p>CoL against <i>P. aeruginosa</i> was 50 µg/mL. CoL and NiL against <i>S. pyogenes</i> represented 62.5 µg/mL.</p>	<p>The ZnL complex has notable efficacy, while NiL and CuL complexes depict moderate efficacy.</p>	<p>The CuL and ZnL complexes have superior anti-inflammatory activity.</p>	Our findings

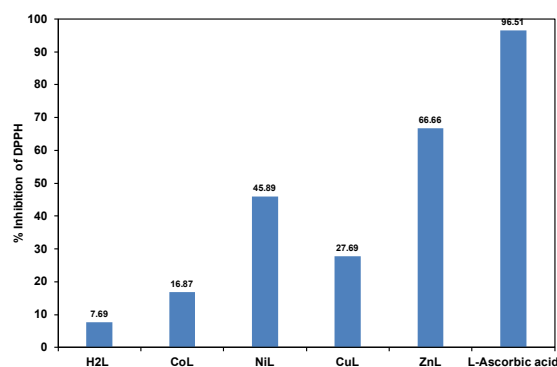


Figure 4. Graphical representation of the antioxidant activity of the synthesized compounds.

The compound H₂L displayed a half maximum inhibitory concentration (IC₅₀) value of 2.43 µg/mL, while all complexes demonstrated enhanced bioactivity against malarial parasites, with IC₅₀ values ranging from 0.5 to 1.98 µg/mL. The ideas of lipophilicity and chelation help to explain why complexes are more effective against malaria than ligands. Lipophilicity increases cell membrane permeability, allowing passive transport across the membrane and increasing intracellular accumulation, which alters cellular metabolic activity, resulting in cytoplasmic leakage and cell death [22,71]. CuL and ZnL complexes of the Schiff base ligand demonstrated significant effectiveness, with IC₅₀ values of 0.5 and 0.75 µg/mL, respectively. The CoL and NiL complexes showed moderate activity, with IC₅₀ values of 1.24 and 1.98 µg/mL, respectively. The antimalarial efficacy of the obtained complexes and ligand can be arranged as follows; CuL > ZnL > CoL > NiL > H₂L. In this study, we compared the IC₅₀ values of our synthesized compounds with similar moieties from the literature, as shown in Table 2, indicating that our named molecules showed superior antimalarial activity.

3.4. Antioxidant studies

The radicals generated during oxidative metabolism are known as reactive oxygen species (ROS). These species possess the ability to oxidize biomolecules such as proteins, carbohydrates, lipids, nucleic acids, and polyunsaturated fatty acids, thus causing oxidative damage such as membrane dysfunction, enzymatic inactivation, and DNA breakage. The antioxidants have the capability to obstruct or delay the oxidation of biomolecules, along with the generation of free radicals. Therefore, the supply of antioxidant-rich drugs is

important to our body to avoid the consequences of oxidative damage [17]. Oxidative damage is the main cause of severe ailments such as cancer, heart disease, Parkinson's, etc. [75]. Therefore, there is a vital requirement to expand the research on the development of antibiotic drugs [71]. To contribute to the field of antioxidant drug development research, we tested the antioxidant properties of our synthesized compounds using a DPPH radical assay and compared them to standard L-ascorbic acid. Figure 4 illustrates the graphical representation of antioxidant activity. The cumulative bioactivity data shows that all complexes exceed the bioefficacy of the ligand. Among the complexes, the ZnL complex has notable efficacy, whereas the NiL and CuL complexes show moderate efficacy. However, the CoL and CuL complexes illustrate weak bioactivity. Thus, the bioactivity trend of the compound is H₂L < CoL < CuL < NiL < ZnL < L-ascorbic acid. This could be explained by the compound's ability to deform the structure of free radicals via hydrogen atom donation [17, 76]. As depicted in Table 1, extensive literature reviews have consistently affirmed the anti-oxidative properties of Salen Schiff base metal complexes. In comparison with the other reported molecules, our compounds exhibit remarkable to moderate antioxidant potential.

3.5. Anti-inflammatory activity studies

Within the body, inflammation serves as an alarm system, signalling potential damage or abnormalities to individuals. Chronic pain or inflammation significantly affects people's quality of life, as nearly everyone experiences inflammation at some point, whether it is chronic or acute.

Table 2. Comparison of antimalarial activity with relevant moieties.

Compound	Structure	IC ₅₀ value	Reference
6		IC ₅₀ (6) = 2.29 μM	[72]
6a		IC ₅₀ (6a) = 0.96±0.02 μM	[22]
2 and 3		IC ₅₀ (2) = 9.88±0.23 μM IC ₅₀ (3) = 1.06±0.01 μM	[73]
Co(L ₁)(L ₂)Cl ₂ ·3H ₂ O Zn(L ₁)(L ₂)Cl Cd(L ₁)(L ₂)Cl ₃		IC ₅₀ (Co complex) = 0.92 μM IC ₅₀ (Zn complex) = 0.98 μM IC ₅₀ (Cd complex) = 0.98 μM	[74]
6		IC ₅₀ (6) = 0.95±0.02 μM	[15]
CuL and ZnL		IC ₅₀ (4) = 0.50 μg/mL IC ₅₀ (5) = 0.75 μg/mL	Our findings

Therefore, treating pain, mainly chronic pain, is extremely intricate and therefore it is crucial to synthesize new anti-inflammatory drugs with fewer adverse effects [17]. Several prolonged inflammatory diseases were treated with non-steroidal anti-inflammatory drugs. These drugs generally impede the formation of prostaglandins, while other pro-inflammatory drugs prohibit the cyclooxygenase (COX) enzyme formation, which is responsible for converting arachidonic acid into prostaglandins. Reducing the formation of prostaglandins and arachidonic acid regulates the immune response and anti-inflammatory properties [17-19]. The anti-inflammatory efficacy of the synthesized ligand and its metal complexes is shown in Figure 5 with the standard drug diclofenac sodium. The findings revealed that all metal complexes showed significant bioactivity compared to that of the free Schiff base ligand. However, in comparison to sodium diclofenac, both the complexes and the ligand exhibited a lower percentage of inhibition. CuL and ZnL complexes were shown to be better than NiL and CoL complexes. The anti-inflammatory efficiencies of compounds have the following sequence: CuL > ZnL > NiL >

CoL > H₂L. Many studies have confirmed the anti-inflammatory effect of metal complexes containing the Salen Schiff base ligand, notably those combining Zn(II) and Cu(II) metals, our compounds have moderate anti-inflammatory activity compared to other similar compounds (Table 1).

3.6. Molecular docking studies

We performed a docking investigation employing the Glide module (Schrodinger Inc., USA) to determine the correlation between theoretical and experimental findings. The ligand and its corresponding metal complexes were docked to receptor proteins, including *S. pyogenes* cysteine protease SpeB, and *P. falciparum* lactate dehydrogenase. Table 3 shows the results of the docking investigation, and Figures 6 and 7 show the 3D docking structure of both receptor proteins. As seen in Figures 6 and 7, a higher negative docking score is a crucial characteristic in the drug development process, as it suggests a significant binding affinity between a molecule and the target protein.

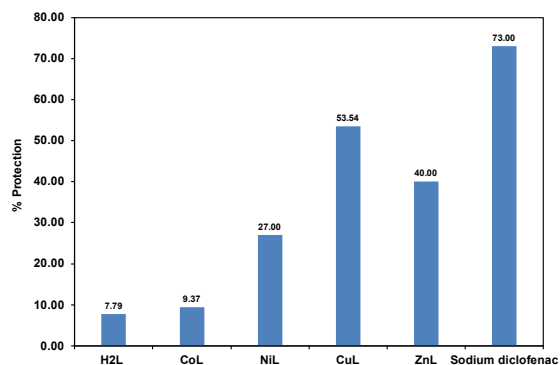


Figure 5. Anti-inflammatory activities of the synthesized compounds.

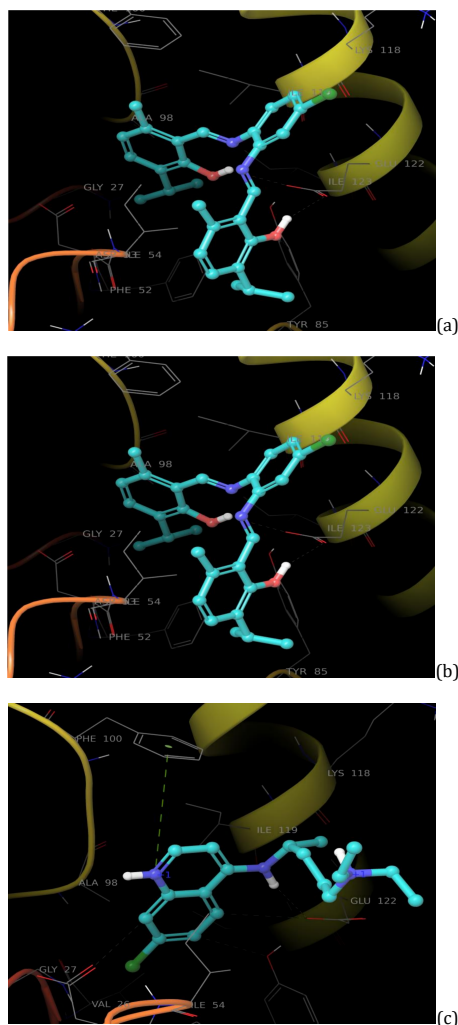


Figure 6. 3D structure of the interaction of ligand, CuL, and chloroquine with *P. falciparum* lactate dehydrogenase.

The molecular docking analysis demonstrated that the Salen-type Schiff base ligand had a greater negative binding energy for both receptor proteins. It specifically engages in hydrogen bond interactions with the cysteine protease SpeB receptor protein's Gly-339 amino acids, resulting in a docking score of -6.138 kcal/mol. Additionally, it has a strong hydrogen bond interaction with the lactate dehydrogenase receptor protein's Glu-122, with a docking score of -8.23 kcal/mol, that is similar to that of conventional chloroquine. Among the synthesized metal complexes, CoL shows a robust hydrogen bond interaction with the Cys-192 amino acid of the cysteine

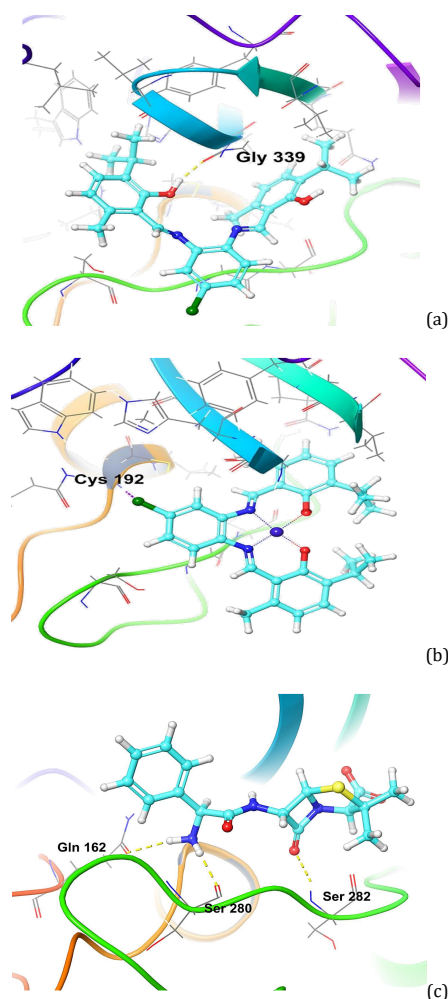
protease SpeB protein through a chlorine atom, resulting in a higher docking score (-5.04 kcal/mol) compared to other metal complexes. Interestingly, the CuL and ZnL complexes exhibited a robust π - π stacking interaction with the hydrophobic Phe-100 amino acid of *P. falciparum* lactate dehydrogenase, producing docking scores of -8.26 and -7.74 kcal/mol, respectively. In general, all generated complexes had a higher docking score (-8.26 to -6.786 kcal/mol) compared to the malarial standard drug chloroquine (-5.104 kcal/mol).

Table 3. Docking score of the synthesized compounds towards *S. pyogenes* cysteine protease SpeB and *P. falciparum* lactate dehydrogenase by SP docking method.

Protein receptor	<i>S. pyogenes</i> cysteine protease SpeB			<i>P. falciparum</i> lactate dehydrogenase		
	Docking score	Glide emodel	Glide energy	Docking score	Glide emodel	Glide energy
Ampicillin	-7.026	-56.322	-40.235	-	-	-
Chloroquine	-	-	-	-5.104	-43.674	-31.152
H ₂ L	-6.138	-56.436	-43.888	-8.231	-88.033	-52.714
CoL	-5.040	-46.305	-36.006	-6.786	-51.346	-39.562
NiL	-3.726	-42.215	-35.496	-7.171	-64.562	-46.831
CuL	-3.156	-38.124	-30.154	-7.738	-78.228	-49.944
ZnL	-4.812	-46.011	-36.442	-8.260	-84.363	-50.770

Table 4. Thermal parameters and dipole moment (Debye) of compound H₂L and its CoL, NiL, CuL, and ZnL complexes.

Parameters	H ₂ L	CoL	NiL	CuL	ZnL
E_{rot} (Hartree)	-1805.20	-3185.98	-3311.58	-3443.76	-3582.61
Total dipole moment (Debye)	4.46771	2.07914	4.00309	4.13683	2.85367
E_{HOMO} (eV)	-5.4612	-12.1959	-12.2803	-12.3646	-12.2150
E_{LUMO} (eV)	-1.7496	-10.8326	-11.3524	-10.5497	-11.3361
ΔE (eV)	3.7116	1.3633	0.9279	1.8149	0.8789
Electronegativity (χ) (eV)	3.6054	11.5142	11.8163	11.4571	11.7755
Global hardness (η) (eV)	1.8558	0.6816	0.4639	0.9074	0.4394
Global softness (δ) (eV)	0.5388	1.4671	2.1556	1.1020	2.2758
Electrophilicity (ω) (eV)	3.5022	97.2541	150.4900	72.3300	157.7800
Ionization potential ($I = -E_{\text{HOMO}}$) (eV)	5.4612	12.1959	12.2803	12.3646	12.2150
Electron affinity ($A = -E_{\text{LUMO}}$) (eV)	1.7496	10.8326	11.3524	10.5497	11.3361

**Figure 7.** 3D structure of the interaction of ligand, CoL and ampicillin with *S. pyogenes* cysteine protease SpeB.

Higher docking scores of the synthesized compounds against *P. falciparum* lactate dehydrogenase indicated that all compounds have significant binding interactions with malarial receptor proteins. This intriguing result emphasizes the need for further investigation into the potential applicability of our compounds in drug development.

3.7. Density functional theory studies

Through TD-DFT calculations in the gas phase, the DFT analysis was used to optimize the geometry and find the least energy conformations from which several thermochemical properties, including total energy, dipole moment, HOMO, and LUMO, are calculated.

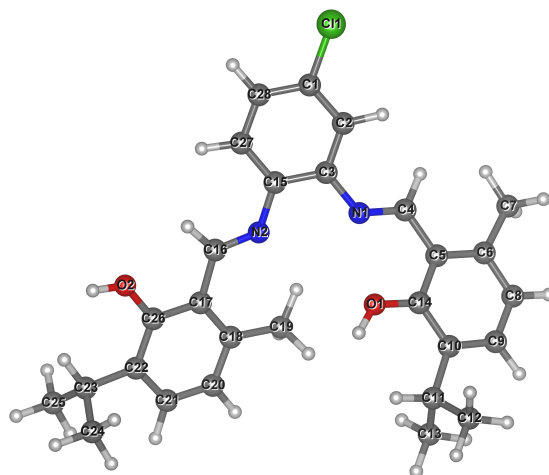


Figure 8. Optimized geometry of the ligand, H₂L.

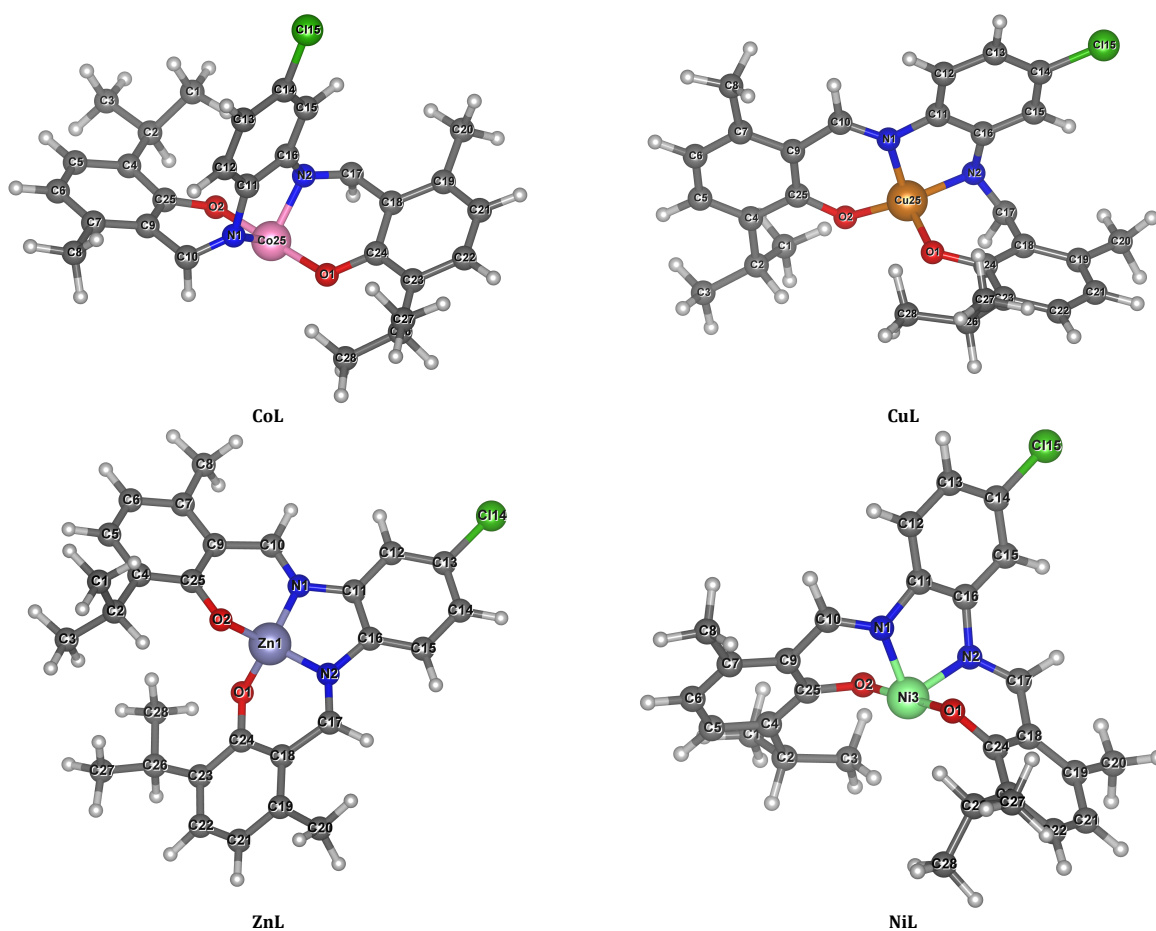


Figure 9. Optimized geometries of CoL, NiL, CuL, and ZnL complexes.

Figures 8 and 9 shows the optimized shape of the ligand and its equivalent metal complexes. Table 4 highlights the dipole moment and total energies (E_{tot}) of the compounds produced.

The total energy values of the H₂L ligand and its CoL, NiL, CuL, and ZnL complexes were determined as follows: -1805.20, -3185.98, -3311.58, -3443.76, -3582.61 (Hartree), respectively. It should be noted that compared to the ligand (H₂L), all metal complexes showed higher negative energy levels, indicating that they are all more stable than the ligand [59]. Among the metal complexes, the ZnL complex was the most stable due to

its higher negative total energy (-3582.6 Hartree), whereas the CoL complex was less stable due to its lower negative total energy (-3185.98 Hartree). The dipole moment plays a crucial role in determining the binding interactions of synthesized compounds with receptor proteins. Among the compounds synthesized, the ligand (H₂L) showed the highest polarity with a dipole moment of $\mu=4.46771$ Debye, while CoL exhibited the lowest polarity with a dipole moment of $\mu=2.07914$ Debye.

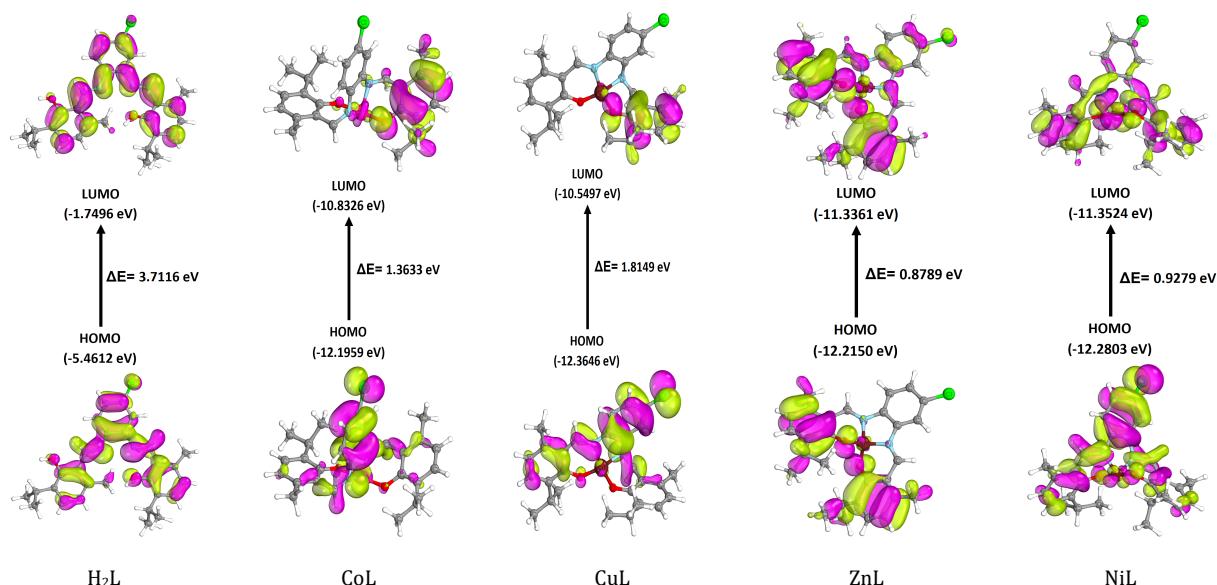


Figure 10. HOMO-LUMO energy gap of ligand and its metal complexes.

Understanding the concept of polarity is particularly important to predict the lipophilicity of compounds, which determines their ability to penetrate the lipophilic membrane of microorganisms [78].

3.8. Frontier molecular orbital's and chemical reactivity parameters

The Frontier molecular orbitals (FMO) of the synthesized ligand and its metal complexes are represented in Figure 10. HOMO is the highest occupied molecular orbital, while LUMO is the lowest occupied molecular orbital. The electron occupation in HOMO and LUMO is investigated to predict the chemical reactivity attributes of the synthesized ligand and its corresponding metal complexes [79]. HOMO is an electron donor, while LUMO is an electron acceptor. The HOMO-LUMO energy difference is recognized as an energy gap, which is an essential parameter for the determination of the stability and reactivity of compounds. The small value of the HOMO-LUMO energy difference (ΔE) is due to its high degree of intramolecular charge transfer from the electron donor side to the acceptor side [80].

The chemical reactivity parameters of the synthesized Salen-type ligand H₂L and its metal complexes are represented in Table 4. Analysis of the frontier molecular orbital data implies that complexation results in a reduction in the energy gap of the compounds. This smaller energy gap in complexes signifies higher polarity, conductivity, high biological efficacy, and kinetically low stability [81]. Explicitly, the ligand primarily displays the highest energy gap ($\Delta E = 3.7$ eV), while its analogous metal complexes demonstrate a decrease in energy gap ($\Delta E = 0.87$ - 1.3 eV). The higher reactivity of the metal complexes is attributed to their smaller energy gap. However, the enhanced stability of the ligand is attributed to its higher energy gap. The stability order of the compounds on the basis of the energy gap is as follows: H₂L > CuL > CoL > NiL > ZnL, and the reactivity order is as follows: ZnL > NiL > CoL > CuL > H₂L. The nucleophilic potential of compounds is determined by the higher value of E_{HOMO} , whereas the electrophilic potential of compounds is determined by the lower value of E_{LUMO} [82]. A higher value of E_{HOMO} demonstrates that the molecule has a higher electron-donating capability, while the lowest value of E_{LUMO} demonstrates that molecules have a higher electron-accepting potential [83]. The compound H₂L shows a more

reactive HOMO, whereas the metal complexes have a less reactive HOMO. Metal complexes demonstrate LUMO with less energy, and the ligand demonstrates LUMO with high energy. According to Koopman's theorem [84], global reactivity parameters such as global softness (δ), global hardness (η), ionization potential ($I = -E_{\text{HOMO}}$), electron affinity ($A = -E_{\text{LUMO}}$), electronegativity (χ), and electrophilicity (ω) can be calculated from the energies of HOMO and LUMO [84]. Molecules with a higher electronegativity index (χ) manifest acidic attributes, while compounds with a smaller electronegativity (χ) showcase their basic nature. In accordance with the electronegativity values, all complexes demonstrate acidic nature, while the ligand exhibits basic nature. The prevention of charge transfer capability in compounds is recognized as global hardness, while the electron transfer ability of compounds is called global softness. Here, the compound H₂L exhibits an elevated global hardness, while the complexes have enhanced global softness parameters. Softer molecules are more polarizable compared to harder molecules. Ligand H₂L is a good nucleophile due to its lower electrophilicity parameter, while metal complexes are good electrophiles due to their higher electrophilicity parameters. In particular, ZnL acts as a proficient electrophile because of its elevated electrophilicity index. All metal complexes have higher electron-accepting ability, while the ligand has higher electron-donating ability. The ionization potential is determined by the chemical potential and electronegativity parameters of the compounds. A higher value of the chemical potential manifests a greater ability to lose electrons. The compound CuL has the highest ionization potential ($I = 12.36$ eV), whereas the Salen-Schiff base ligand has the lowest ionization potential ($I = 5.4$ eV). All these parameters can greatly influence the binding affinity of compounds to the active sites of proteins. All complexes demonstrate higher antibacterial, antioxidant, antimalarial, and anti-inflammatory bioefficacy compared to those of the ligand, owing to their small energy gap, negative HOMO, and higher softness values. Especially among the synthesized complexes, the higher biological efficacy of CuL can be explained on the basis of the most negative HOMO and the least negative LUMO.

4. Conclusion

We have effectively synthesized a novel quadridentate Schiff base ligand (H₂L = 6, 6'-((4-chloro-1, 2-phenylene)bis

(azanylylidene)) bis(methanylylidene)) bis(2-isopropyl-5-methylphenol)), along with its corresponding metal complexes: CoL, NiL, CuL, and ZnL. The spectroscopic characterization data of the synthesized complexes indicate that the metal ions coordinate to the ligand *via* nitrogen and oxygen atoms of the ligand in a 1:1 stoichiometric ratio. The DFT findings show that ligands are more stable, while complexes are more reactive. The stability order of the complexes is shown below: CuL > CoL > NiL > ZnL. The biological investigation of the synthesized compounds indicates that all complexes are more effective than their parent ligand (H₂L). According to DFT studies complexes have a smaller energy gap, the most negative HOMO, and greater softness values, which contribute to their increased effectiveness. The CuL complex has remarkable antimalarial and anti-inflammatory activity, whereas ZnL has enhanced antioxidant and antibacterial effectiveness. Compared to conventional ampicillin drug (MIC = 100 µg/mL), all synthesized complexes (MIC = 62.5-100 µg/mL) have shown outstanding potency against *S. pyogenes* bacteria. Additionally, the CoL complex (MIC = 50 µg/mL) demonstrated superior efficacy against *P. aeruginosa*. Moreover, the most effective binding interactions of the synthesized complexes with the most active sites of lactate dehydrogenase and cysteine protease SpeB have been revealed by molecular docking analysis.

Acknowledgements

The authors express their gratitude to the Department of Science and Technology under the Fund for Improvement of Science and Technology Infrastructure (FIST) program (Project number: SR/FIST-415/2018). The authors are also grateful to the esteemed Management and Principal of Shri Neminath Jain Brahmacharyashram Karmvir Keshavlalji Harakchandji Abad Arts, Shriman Motilalji Giridharilalji Lodha Commerce and Shriman P. H. Jain Science College Chandwad as well as the School of Chemical Sciences, Kavayitri Bahinabai Chaudhari North Maharashtra University, Jalgaon, for providing research facilities. Additionally, authors are also grateful to Sophisticated Analytical Instrumentation Facility of Punjab University, for providing characterization facilities.

Disclosure statement

Conflict of interest: The authors declare that they have no conflict of interest. Author contribution: All authors contributed equally to this work.

Ethical approval: All ethical guidelines have been adhered to.

Sample availability: Samples of the compounds are available from the author.

CRedit authorship contribution statement

Conceptualization: Minakshree Abhijeet Todarwal; Methodology: Minakshree Abhijeet Todarwal; Validation: Minakshree Abhijeet Todarwal; Formal Analysis: Ratnamala Subhash Bendre; Investigation: Ratnamala Subhash Bendre; Resources: Ratnamala Subhash Bendre; Data Curation: Rakesh Suresh Sancheti; Writing - Original Draft: Minakshree Abhijeet Todarwal; Writing - Review and Editing: Samina Karimkha Tadavi, Ratnamala Subhash Bendre; Visualization: Rakesh Suresh Sancheti; Supervision: Ratnamala Subhash Bendre.

ORCID and Email

Minakshree Abhijeet Todarwal

 jainminakshree@gmail.com

 <https://orcid.org/0000-0001-6646-7672>

Samina Karimkha Tadavi

 saminatadavi30@gmail.com

 <https://orcid.org/0000-0002-2772-0329>

Rakesh Suresh Sancheti

 sanchet83@gmail.com

 <https://orcid.org/0000-0002-9903-6649>

Ratnamala Subhash Bendre

 bendrrs@gmail.com

 <https://orcid.org/0000-0001-6987-9912>

References

- Gogoi, H. P.; Barman, P. Salophen type ONNO donor Schiff base complexes: Synthesis, characterization, bioactivity, computational, and molecular docking investigation. *Inorganica Chim. Acta* **2023**, *556*, 121668.
- Vernekar, B. K.; Sawant, P. S. Interaction of metal ions with Schiff bases having N2O2 donor sites: Perspectives on synthesis, structural features, and applications. *Results Chem.* **2023**, *6*, 101039.
- Hosny, S.; El-Baki, R. F. A.; El-Wahab, Z. H. A.; Gouda, G. A.; Saddik, M. S.; Aljuhani, A.; Abu-Dief, A. M. Development of novel nano-sized imine complexes using Coriandrum sativum extract: Structural elucidation, non-isothermal kinetic study, theoretical investigation and pharmaceutical applications. *Int. J. Mol. Sci.* **2023**, *24*, 14259.
- Abu-Dief, A. M.; El-Khatib, R. M.; Aljohani, F. S.; Al-Abdulkarim, H. A.; Alzahrani, S.; El-Sarrag, G.; Ismael, M. Synthesis, structural elucidation, DFT calculation, biological studies and DNA interaction of some aryl hydrazone Cr³⁺, Fe³⁺, and Cu²⁺ chelates. *Comput. Biol. Chem.* **2022**, *97*, 107643.
- Abu-Dief, A. M.; El-khatib, R. M.; Sayed, S. M. E.; Alzahrani, S.; Alkhatib, F.; El-Sarrag, G.; Ismael, M. Tailoring, structural elucidation, DFT calculation, DNA interaction and pharmaceutical applications of some aryl hydrazone Mn(II), Cu(II) and Fe(III) complexes. *J. Mol. Struct.* **2021**, *1244*, 131017.
- Aljohani, E. T.; Shehata, M. R.; Alkhatib, F.; Alzahrani, S. O.; Abu-Dief, A. M. Development and structure elucidation of new VO₂⁺, Mn₂⁺, Zn₂⁺, and Pd₂⁺ complexes based on azomethine ferrocenyl ligand: DNA interaction, antimicrobial, antioxidant, anticancer activities, and molecular docking. *Appl. Organomet. Chem.* **2021**, *35*, e6154.
- Aljohani, E. T.; Shehata, M. R.; Abu-Dief, A. M. Design, synthesis, structural inspection of Pd²⁺, VO₂⁺, Mn²⁺, and Zn²⁺chelates incorporating ferrocenyl thiophenol ligand: DNA interaction and pharmaceutical studies. *Appl. Organomet. Chem.* **2021**, *35*, e6169.
- Abdel-Rahman, L. H.; Abu-Dief, A. M.; Moustafa, H.; Abdel-Mawgoud, A. A. H. Design and nonlinear optical properties (NLO) using DFT approach of new Cr(III), VO(II), and Ni(II) chelates incorporating tridentate imine ligand for DNA interaction, antimicrobial, anticancer activities and molecular docking studies. *Arab. J. Chem.* **2020**, *13*, 649–670.
- Abdel-Rahman, L. H.; Abu-Dief, A. M.; Hassan Abdel-Mawgoud, A. A. Development, structural investigation, DNA binding, antimicrobial screening and anticancer activities of two novel quadri-dentate VO(II) and Mn(II) mononuclear complexes. *J. King Saud Univ. Sci.* **2019**, *31*, 52–60.
- Abdel-Rahman, L. H.; Adam, M. S. S.; Abu-Dief, A. M.; Moustafa, H.; Basha, M. T.; Aboraia, A. S.; Al-Farhan, B. S.; Ahmed, H. E.-S. Synthesis, theoretical investigations, biocidal screening, DNA binding, *in vitro* cytotoxicity and molecular docking of novel Cu(II), Pd(II) and Ag(I) complexes of chlorobenzylidene Schiff base: Promising antibiotic and anticancer agents. *Appl. Organomet. Chem.* **2018**, *32*, e4527.
- Abdel-Rahman, L. H.; Abu-Dief, A. M.; Aboelez, M. O.; Hassan Abdel-Mawgoud, A. A. DNA interaction, antimicrobial, anticancer activities and molecular docking study of some new VO(II), Cr(III), Mn(II) and Ni(II) mononuclear chelates encompassing quaridentate imine ligand. *J. Photochem. Photobiol. B* **2017**, *170*, 271–285.
- Abdel-Rahman, L. H.; Abu-Dief, A. M.; El-Khatib, R. M.; Abdel-Fatah, S. M. Some new nano-sized Fe(II), Cd(II) and Zn(II) Schiff base complexes as precursor for metal oxides: Sonochemical synthesis, characterization, DNA interaction, *in vitro* antimicrobial and anticancer activities. *Bioorg. Chem.* **2016**, *69*, 140–152.
- Adly, O. M. I.; Taha, A.; Fahmy, S. A. Synthesis, spectral characterization, molecular modeling and antimicrobial activity of new potentially N2O2 Schiff base complexes. *J. Mol. Struct.* **2013**, *1054–1055*, 239–250.
- Sharma, V.; Arora, E. K.; Cardoza, S. Synthesis, antioxidant, antibacterial, and DFT study on a coumarin based salen-type Schiff base and its copper complex. *Chem. Pap.* **2016**, *70*, 1493–1502.
- Das, K.; Shetty, M. G.; Melanthota, S. K.; Sundara, B. K.; Kar, S.; Massera, C.; Garrriba, E.; Datta, A.; Mazumder, N. Structural elucidation of a Mn(III) derivative anchored with a tetradentate Schiff base precursor: *in vitro* cytotoxicity study. *Chem. Pap.* **2023**, *77*, 1989–1998.
- Damercheli, M.; Dayyani, D.; Behzad, M.; Mehravi, B.; Shafiee Ardestani, M. New salen-type manganese(III) Schiff base complexes derived from *meso*-1,2-diphenyl-1,2-ethylenediamine: *In vitro* anticancer activity, mechanism of action, and molecular docking studies. *J. Coord. Chem.* **2015**, *68*, 1500–1513.
- Singh, A.; Gogoi, H. P.; Barman, P.; Das, A.; Pandey, P. Tetracoordinated ONNO donor purine-based Schiff base and its metal complexes: Synthesis, characterization, DNA binding, theoretical studies, and bioactivities. *Appl. Organomet. Chem.* **2022**, *36*, e6852.
- Abdel-Rahman, L. H.; Ismail, N. M.; Ismael, M.; Abu-Dief, A. M.; Ahmed, E. A.-H. Synthesis, characterization, DFT calculations and biological studies of Mn(II), Fe(II), Co(II) and Cd(II) complexes based on a

- tetradentate ONNO donor Schiff base ligand. *J. Mol. Struct.* **2017**, *1134*, 851–862.
- [19]. Abdel-Rahman, L. H.; Adam, M. S. S.; Al-Zaqri, N.; Shehata, M. R.; El-Sayed Ahmed, H.; Mohamed, S. K. Synthesis, characterization, biological and docking studies of ZrO(II), VO(II) and Zn(II) complexes of a halogenated tetra-dentate Schiff base. *Arab. J. Chem.* **2022**, *15*, 103737.
- [20]. Ariyaefar, M.; Amiri Rudbari, H.; Sahihi, M.; Kazemi, Z.; Kajani, A. A.; Zali-Boeini, H.; Kordestani, N.; Bruno, G.; Gharaghani, S. Chiral halogenated Schiff base compounds: green synthesis, anticancer activity and DNA-binding study. *J. Mol. Struct.* **2018**, *1161*, 497–511.
- [21]. World malaria report 2022. <https://www.who.int/teams/global-malaria-programme/reports/world-malaria-report-2022> (accessed January 26, 2024).
- [22]. Dalal, M.; Antil, N.; Kumar, B.; Devi, J.; Garg, S. Exploring the novel aryltellurium(IV) complexes: Synthesis, characterization, antioxidant, antimicrobial, antimalarial, theoretical and ADMET studies. *Inorg. Chem. Commun.* **2024**, *159*, 111743.
- [23]. Anacona, J. R.; Santaella, J.; Al-shemary, R. K. R.; Amenta, J.; Otero, A.; Ramos, C.; Celis, F. Ceftriaxone-based Schiff base transition metal(II) complexes. Synthesis, characterization, bacterial toxicity, and DFT calculations. Enhanced antibacterial activity of a novel Zn(II) complex against *S. aureus* and *E. coli*. *J. Inorg. Biochem.* **2021**, *223*, 111519.
- [24]. Ramesh, G.; Daravath, S.; Swathi, M.; Sumalatha, V.; Shiva Shankar, D.; Shivaraj Investigation on Co(II), Ni(II), Cu(II) and Zn(II) complexes derived from quadridentate salen-type Schiff base: Structural characterization, DNA interactions, antioxidant proficiency and biological evaluation. *Chem. Data Coll.* **2020**, *28*, 100434.
- [25]. Farag, A. M.; Guan, T. S.; Osman, H.; Majid, A. M. S. A.; Iqbal, M. A.; Ahamed, M. B. K. Synthesis of metal(II) [M = Cu, Mn, Zn] Schiff base complexes and their Pro-apoptotic activity in liver tumor cells via caspase activation. *Med. Chem. Res.* **2013**, *22*, 4727–4736.
- [26]. Kargar, H.; Adabi Ardakani, A.; Munawar, K. S.; Ashfaq, M.; Tahir, M. N. Nickel(II), copper(II) and zinc(II) complexes containing symmetrical Tetradentate Schiff base ligand derived from 3,5-diiodosalicylaldehyde: Synthesis, characterization, crystal structure and antimicrobial activity. *J. Iran. Chem. Soc.* **2021**, *18*, 2493–2503.
- [27]. Abdel Aziz, A. A.; Ramadan, R. M.; Sidqi, M. E.; Sayed, M. A. Structural characterisation of novel mononuclear Schiff base metal complexes, DFT calculations, molecular docking studies, free radical scavenging, DNA binding evaluation and cytotoxic activity. *Appl. Organomet. Chem.* **2023**, *37*, e6954.
- [28]. Bendre, R. S.; Tadavi, S. K.; Patil, M. M. Synthesis, crystal structures and biological activities of transition metal complexes of a salen-type ligand. *Transit. Met. Chem.* **2018**, *43*, 83–89.
- [29]. Subhash; Chaudhary, A.; Mamta; Jyoti Synthesis, structural characterization, thermal analysis, DFT, biocidal evaluation and molecular docking studies of amide-based Co(II) complexes. *Chem. Pap.* **2023**, *77*, 5059–5078.
- [30]. Tople, M. S.; Patel, N. B.; Patel, P. P.; Purohit, A. C.; Ahmad, I.; Patel, H. An in silico-in vitro antimalarial and antimicrobial investigation of newer 7-chloroquinoline based Schiff-bases. *J. Mol. Struct.* **2023**, *1271*, 134016.
- [31]. Desjardins, R. E.; Canfield, C. J.; Haynes, J. D.; Chulay, J. D. Quantitative assessment of antimalarial activity in vitro by a semiautomated microdilution technique. *Antimicrob. Agents Chemother.* **1979**, *16*, 710–718.
- [32]. Gandhidasan, R.; Thamarachelvan, A.; Baburaj, S. Anti inflammatory action of Lannea coromandelica by HRBC membrane stabilization. *Fitoterapia* **1991**, *62*, 81–83.
- [33]. Anosike, C. A.; Obidoa, O.; Ezeanyika, L. U. S. Membrane stabilization as a mechanism of the anti-inflammatory activity of methanol extract of garden egg (*Solanum aethiopicum*). *Daru* **2012**, *20*, 76 <https://doi.org/10.1186/2008-2231-20-76>.
- [34]. Krishna, G. A.; Dhanya, T. M.; Shanty, A. A.; Raghu, K. G.; Mohanan, P. V. Transition metal complexes of imidazole derived Schiff bases: Antioxidant/anti-inflammatory/antimicrobial/enzyme inhibition and cytotoxicity properties. *J. Mol. Struct.* **2023**, *1274*, 134384.
- [35]. Ejidike, I. P.; Ajibade, P. A. Synthesis, characterization, and in vitro antioxidant and anticancer studies of ruthenium(III) complexes of symmetric and asymmetric tetradentate Schiff bases. *J. Coord. Chem.* **2015**, *68*, 2552–2564.
- [36]. Al-Amiery, A. A.; Kadhum, A. A. H.; Mohamad, A. B. Antifungal and antioxidant activities of pyrrolidone thiosemicarbazone complexes. *Bioinorg. Chem. Appl.* **2012**, *2012*, 1–6.
- [37]. Bathula, R.; Muddagoni, N.; Lanka, G.; Dasari, M.; Potlapally, S. Glide docking, AutoDock, binding free energy and drug-likeness studies for prediction of potential inhibitors of cyclin-dependent kinase 14 protein in Wnt signaling pathway. *Biointerface Res. Appl. Chem.* **2021**, *12*, 2473–2488.
- [38]. Patel, H.; Dhangar, K.; Sonawane, Y.; Surana, S.; Karpoornath, R.; Thapliyal, N.; Shaikh, M.; Noolvi, M.; Jagtap, R. In search of selective 11 β -HSD type 1 inhibitors without nephrotoxicity: An approach to resolve the metabolic syndrome by virtual based screening. *Arab. J. Chem.* **2018**, *11*, 221–232.
- [39]. Wang, A. Y.; González-Páez, G. E.; Wolan, D. W. Identification and co-complex structure of a new *S. pyogenes* SpeB small molecule inhibitor. *Biochemistry* **2015**, *54*, 4365–4373.
- [40]. Radwan, H. A.; Ahmad, I.; Othman, I. M. M.; Gad-Elkareem, M. A. M.; Patel, H.; Aouadi, K.; Snoussi, M.; Kadri, A. Design, synthesis, in vitro anticancer and antimicrobial evaluation, SAR analysis, molecular docking and dynamic simulation of new pyrazoles, triazoles and pyridazines based isoxazole. *J. Mol. Struct.* **2022**, *1264*, 133312.
- [41]. Mazri, R.; Ouassaf, M.; Kerassa, A.; Alhatlani, B. Y. Exploring potential therapeutics: Targeting dengue virus NS5 through molecular docking, ADMET profiling, and DFT analysis. *Chemical Physics Impact* **2024**, *8*, 100468.
- [42]. Harder, E.; Damm, W.; Maple, J.; Wu, C.; Rebol, M.; Xiang, J. Y.; Wang, L.; Lupyan, D.; Dahlgren, M. K.; Knight, J. L.; Kaus, J. W.; Cerutti, D. S.; Krilov, G.; Jorgensen, W. L.; Abel, R.; Friesner, R. A. OPLS3: A force field providing broad coverage of drug-like small molecules and proteins. *J. Chem. Theory Comput.* **2016**, *12*, 281–296.
- [43]. Ahmad, I.; Shaikh, M.; Surana, S.; Ghosh, A.; Patel, H. p38 α MAP kinase inhibitors to overcome EGFR tertiary C797S point mutation associated with osimertinib in non-small cell lung cancer (NSCLC): emergence of fourth-generation EGFR inhibitor. *J. Biomol. Struct. Dyn.* **2022**, *40*, 3046–3059.
- [44]. Ahmad, I.; Pawara, R. H.; Girase, R. T.; Pathan, A. Y.; Jagatap, V. R.; Desai, N.; Ayipo, Y. O.; Surana, S. J.; Patel, H. Synthesis, molecular modeling study, and quantum-chemical-based investigations of isoindoline-1,3-diones as antimycobacterial agents. *ACS Omega* **2022**, *7*, 21820–21844.
- [45]. Ahmad, I.; Pawara, R.; Patel, H. In silico toxicity investigation of Methaqualone's conjunctival, retinal, and gastrointestinal hemorrhage by molecular modelling approach. *Mol. Simul.* **2022**, *48*, 1639–1649.
- [46]. Girase, R.; Ahmad, I.; Pawara, R.; Patel, H. Optimizing cardio, hepato and phospholipidosis toxicity of the Bedaquiline by chemoinformatics and molecular modelling approach. *SAR QSAR Environ. Res.* **2022**, *33*, 215–235.
- [47]. Chalkha, M.; Nour, H.; Chebbac, K.; Nakkabi, A.; Bahsis, L.; Bakhouch, M.; Akhazzane, M.; Bourass, M.; Chitita, S.; Bin Jardan, Y. A.; Augustyniak, M.; Bourhia, M.; Aboul-Soud, M. A. M.; El Yazidi, M. Synthesis, characterization, DFT mechanistic study, antimicrobial activity, molecular modeling, and ADMET properties of novel pyrazole-isoxazoline hybrids. *ACS Omega* **2022**, *7*, 46731–46744.
- [48]. Hanwell, M. D.; Curtis, D. E.; Lonie, D. C.; Vandermeersch, T.; Zurek, E.; Hutchison, G. R. Avogadro: an advanced semantic chemical editor, visualization, and analysis platform. *J. Cheminform.* **2012**, *4*, 1–17.
- [49]. Krishnan, R.; Binkley, J. S.; Seeger, R.; Pople, J. A. Self-consistent molecular orbital methods. XX. A basis set for correlated wave functions. *J. Chem. Phys.* **1980**, *72*, 650–654.
- [50]. McLean, A. D.; Chandler, G. S. Contracted Gaussian basis sets for molecular calculations. I. Second row atoms, Z=11–18. *J. Chem. Phys.* **1980**, *72*, 5639–5648.
- [51]. Curtiss, L. A.; McGrath, M. P.; Blaudeau, J.-P.; Davis, N. E.; Binning, R. C., Jr; Radom, L. Extension of Gaussian-2 theory to molecules containing third-row atoms Ga–Kr. *J. Chem. Phys.* **1995**, *103*, 6104–6113.
- [52]. Clark, T.; Chandrasekhar, J.; Spitznagel, G. W.; Schleyer, P. V. R. Efficient diffuse function-augmented basis sets for anion calculations. III. The 3-21+G basis set for first-row elements, Li–F. *J. Comput. Chem.* **1983**, *4*, 294–301.
- [53]. Neese, F. Software update: the ORCA program system, version 4.0. *Wiley Interdiscip. Rev. Comput. Mol. Sci.* **2018**, *8*, e1327.
- [54]. Bühl, M.; Kabrede, H. Geometries of transition-metal complexes from density-functional theory. *J. Chem. Theory Comput.* **2006**, *2*, 1282–1290.
- [55]. Bühl, M.; Reimann, C.; Pantazis, D. A.; Bredow, T.; Neese, F. Geometries of third-row transition-metal complexes from density-functional theory. *J. Chem. Theory Comput.* **2008**, *4*, 1449–1459.
- [56]. Xavier, S.; Periandy, S.; Ramalingam, S. NBO, conformational, NLO, HOMO–LUMO, NMR and electronic spectral study on 1-phenyl-1-propanol by quantum computational methods. *Spectrochim. Acta A Mol. Biomol. Spectrosc.* **2015**, *137*, 306–320.
- [57]. Tweedy, B. G. Plant Extracts with Metal Ions as Potential Antimicrobial Agents. *Phytopatology* **1964**, *55*, 910–918.
- [58]. Beyene, B. B.; Mihirteu, A. M.; Ayana, M. T.; Yibeltal, A. W. Synthesis, characterization and antibacterial activity of metalloporphyrins: Role of central metal ion. *Results Chem.* **2020**, *2*, 100073.
- [59]. Abdalla, E. M.; Abdel Rahman, L. H.; Abdelhamid, A. A.; Shehata, M. R.; Althman, A. A.; Nafady, A. Synthesis, characterization, theoretical studies, and antimicrobial/antitumor potencies of salen and salen/imidazole complexes of Co(II), Ni(II), Cu(II), Cd(II), Al(III) and La(III). *Appl. Organomet. Chem.* **2020**, *34*, e5912.
- [60]. Mansour, A. M. Coordination behavior of sulfamethazine drug towards Ru(III) and Pt(II) ions: Synthesis, spectral, DFT, magnetic, electrochemical and biological activity studies. *Inorganica Chim. Acta* **2013**, *394*, 436–445.
- [61]. Qasem, H. A.; Sayed, F. N.; Feizi-Dehnyayebi, M.; Al-Ghamdi, K.; Omar, I.; Mohamed, G. G.; Abu-Dief, A. M. Development of tripodal imine metal

- chelates: Synthesis, physicochemical inspection, theoretical studies and biomedical evaluation. *Inorg. Chem. Commun.* **2024**, *162*, 112248.
- [62]. El-Remaily, M. A. E. A. A.; Elhady, O.; Abdou, A.; Alhashmialameer, D.; Eskander, T. N. A.; Abu-Dief, A. M. Development of new 2-(Benzo[thiazol-2-ylidino]-2,3-dihydro-1H-imidazol-4-ol) complexes as a robust catalysts for synthesis of thiazole 6-carbonitrile derivatives supported by DFT studies. *J. Mol. Struct.* **2023**, *1292*, 136188.
- [63]. Abu-Dief, A. M.; Said, M. A.; Elhady, O.; Alzahrani, S.; Aljohani, F. S.; Eskander, T. N. A.; Ali El-Remaily, M. A. E. A. Design, structural inspection of some new metal chelates based on benzo[thiazol-pyrimidin-2-ylidene] ligand: Biomedical studies and molecular docking approach. *Inorg. Chem. Commun.* **2023**, *158*, 111587.
- [64]. Abu-Dief, A. M.; El-Dabea, T.; El-Khatib, R. M.; Feizi-Dehnyayeb, M.; Aljohani, F. S.; Al-Ghamdi, K.; Omar Barnawi, I.; Abd El Aleem Ali Ali El-Remaily, M. Synthesis, structural inspection, stoichiometry in solution and DFT calculation of some novel mixed ligand complexes: DNA binding, biomedical applications and molecular docking approach. *J. Mol. Liq.* **2024**, *399*, 124422.
- [65]. Shaghghi, Z.; Kalantari, N.; Kheyrollahpoor, M.; Haëili, M. Optical, electrochemical, thermal, biological and theoretical studies of some chloro and bromo based metal-salophen complexes. *J. Mol. Struct.* **2020**, *1200*, 127107.
- [66]. Tadavi, S. K.; Rajput, J. D.; Bagul, S. D.; Sangshetti, J. N.; Hosamani, A. A.; Bendre, R. S. Crystal structure, spectral characterization and biologically studies of mononuclear transition metal complexes derived from new N2O2 type ligand. *Mod. Chem. Appl.* **2017**, *05*, 1-7. <http://dx.doi.org/10.4172/2329-6798.1000211>.
- [67]. Paul, S.; Barman, P. Exploring diaminomaleonitrile-derived Schiff base ligand and its complexes: Synthesis, characterization, computational insights, biological assessment, and molecular docking. *J. Mol. Struct.* **2024**, *1296*, 136941.
- [68]. Sakthivel, R. V.; Sankudevan, P.; Vennila, P.; Venkatesh, G.; Kaya, S.; Serdaroğlu, G. Experimental and theoretical analysis of molecular structure, vibrational spectra and biological properties of the new Co(II), Ni(II) and Cu(II) Schiff base metal complexes. *J. Mol. Struct.* **2021**, *1233*, 130097.
- [69]. Tadavi, S. K.; Rajput, J. D.; Bagul, S. D.; Hosamani, A. A.; Sangshetti, J. N.; Bendre, R. S. Synthesis, crystal structures, biological screening and electrochemical analysis of some salen-based transition metal complexes. *Res. Chem. Intermed.* **2017**, *43*, 4863-4879.
- [70]. Rieckmann, K. H.; Campbell, G. H.; Sax, L. J.; Ema, J. E. Drug sensitivity of Plasmodium falciparum. *Lancet* **1978**, *311*, 22-23.
- [71]. Kumar, B.; Devi, J.; Dubey, A.; Tufail, A.; Sharma, S. Exploring the antimalarial, antioxidant, anti-inflammatory activities of newly synthesized transition metal(II) complexes bearing thiosemicarbazone ligands: Insights from molecular docking, DFT, MESP and ADMET studies. *Inorg. Chem. Commun.* **2024**, *159*, 111674.
- [72]. Savir, S.; Wei, Z. J.; Liew, J. W. K.; Vythilingam, I.; Lim, Y. A. L.; Saad, H. M.; Sim, K. S.; Tan, K. W. Synthesis, cytotoxicity and antimalarial activities of thiosemicarbazones and their nickel (II) complexes. *J. Mol. Struct.* **2020**, *1211*, 128090.
- [73]. Savir, S.; Liew, J. W. K.; Vythilingam, I.; Lim, Y. A. L.; Tan, C. H.; Sim, K. S.; Lee, V. S.; Maah, M. J.; Tan, K. W. Nickel(II) complexes with polyhydroxybenzaldehyde and O,N,S tridentate thiosemicarbazone ligands: Synthesis, cytotoxicity, antimalarial activity, and molecular docking studies. *J. Mol. Struct.* **2021**, *1242*, 130815.
- [74]. Borhade, S. S.; Tryambake, P. T. Synthesis, characterization, antibacterial, antifungal and antimalarial study of mixed ligand metal complexes derived from azo quinoline with thiosemicarbazone. *Asian J. Chem.* **2021**, *33*, 885-891.
- [75]. Saeidnia, S.; Abdollahi, M. Toxicological and pharmacological concerns on oxidative stress and related diseases. *Toxicol. Appl. Pharmacol.* **2013**, *273*, 442-455.
- [76]. Kizilkaya, H.; Dag, B.; Aral, T.; Genc, N.; Erenler, R. Synthesis, characterization, and antioxidant activity of heterocyclic Schiff bases. *J. Chin. Chem. Soc.* **2020**, *67*, 1696-1701.
- [77]. Munir, A.; Khushal, A.; Saeed, K.; Sadiq, A.; Ullah, R.; Ali, G.; Ashraf, Z.; Ullah Mughal, E.; Saeed Jan, M.; Rashid, U.; Hussain, I.; Mumtaz, A. Synthesis, in-vitro, in-vivo anti-inflammatory activities and molecular docking studies of acyl and salicylic acid hydrazide derivatives. *Bioorg. Chem.* **2020**, *104*, 104168.
- [78]. Shinde, R. A.; Adole, V. A.; Jagdale, B. S.; Desale, B. S. Synthesis, antibacterial and computational studies of Halo Chalcone hybrids from 1-(2,3-Dihydrobenzo[b][1,4]dioxin-6-yl)ethan-1-one. *J. Indian Chem. Soc.* **2021**, *98*, 100051.
- [79]. Rathi, P.; Khanna, R.; Jaswal, V. S. Quantum parameters based study of some heterocycles using density functional theory method: A comparative theoretical study. *J. Chin. Chem. Soc.* **2020**, *67*, 213-217.
- [80]. Meenukuty, M. S.; Mohan, A. P.; Vidya, V. G.; Vijay Kumar, V. G. Synthesis, characterization, DFT analysis and docking studies of a novel Schiff base using 5-bromo salicylaldehyde and β -alanine. *Heliyon* **2022**, *8*, e09600.
- [81]. Sanatkar, T. H.; Khorshidi, A.; Janczak, J. Dinuclear Zn(II) and tetranuclear Co(II) complexes of a tetradentate N2O2 Schiff base ligand: Synthesis, crystal structure, characterization, DFT studies, cytotoxicity evaluation, and catalytic activity toward benzyl alcohol oxidation. *Appl. Organomet. Chem.* **2020**, *34*, e5493.
- [82]. Adole, V. A.; More, R. A.; Jagdale, B. S.; Pawar, T. B.; Chobe, S. S.; Shinde, R. A.; Dhonnar, S. L.; Koli, P. B.; Patil, A. V.; Bukane, A. R.; Gacche, R. N. Microwave prompted solvent-free synthesis of new series of heterocyclic tagged 7-arylidene indanone hybrids and their computational, antifungal, antioxidant, and cytotoxicity study. *Bioorg. Chem.* **2021**, *115*, 105259.
- [83]. Gaber, M.; El-Ghamry, H. A.; Fathalla, S. K. Synthesis, structural identification, DNA interaction and biological studies of divalent Mn, Co and Ni chelates of 3-amino-5-mercapto-1,2,4-triazole azo ligand. *Appl. Organomet. Chem.* **2020**, *34*, e5678.
- [84]. Gritsenko, O. V. Koopmans' theorem and its density-functional-theory analog assessed in evaluation of the red shift of vertical ionization potential upon complexation. *Chem. Phys. Lett.* **2018**, *691*, 178-180.



Copyright © 2024 by Authors. This work is published and licensed by Atlanta Publishing House LLC, Atlanta, GA, USA. The full terms of this license are available at <https://www.eurjchem.com/index.php/eurjchem/terms> and incorporate the Creative Commons Attribution-Non Commercial (CC BY NC) (International, v4.0) License (<http://creativecommons.org/licenses/by-nc/4.0>). By accessing the work, you hereby accept the Terms. This is an open access article distributed under the terms and conditions of the CC BY NC License, which permits unrestricted non-commercial use, distribution, and reproduction in any medium, provided the original work is properly cited without any further permission from Atlanta Publishing House LLC (European Journal of Chemistry). No use, distribution, or reproduction is permitted which does not comply with these terms. Permissions for commercial use of this work beyond the scope of the License (<https://www.eurjchem.com/index.php/eurjchem/terms>) are administered by Atlanta Publishing House LLC (European Journal of Chemistry).